Infectious Disease Modelling 10 (2025) 50–59

Contents lists available at ScienceDirect

Infectious Disease Modelling

journal homepage: www.keaipublishing.com/idm

Forecasting influenza epidemics in China using transmission dynamic model with absolute humidity

Xiaowei Chen [a], Fangfang Tao [b], Yinzi Chen [b], Jian Cheng [c, d], Ying Zhou [e], Xiling Wang [a, f, *]

[a] School of Public Health, Fudan University, Key Laboratory of Public Health Safety, Ministry of Education, Shanghai, China
[b] Institute of Infectious Disease Prevention and Control, Shanghai Municipal Center for Disease Control and Prevention, Shanghai, China
[c] Department of Epidemiology and Biostatistics, School of Public Health, Anhui Medical University, Hefei, China
[d] Anhui Province Key Laboratory of Major Autoimmune Disease, Hefei, China
[e] Shanghai Institute of Aviation Medicine, Ruijin Hospital, Shanghai Jiao Tong University School of Medicine, Shanghai, China
[f] Shanghai Key Laboratory of Meteorology and Health, Shanghai, China

ARTICLE INFO

Article history:
Received 21 June 2024
Received in revised form 9 August 2024
Accepted 9 August 2024
Available online 10 August 2024
Handling Editor: Dr Daihai He

Keywords:
Influenza
Forecasting
Absolute humidity

ABSTRACT

Background: An influenza forecasting system is critical to influenza epidemic preparedness. Low temperature has long been recognized as a condition favoring influenza epidemic, yet it fails to justify the summer influenza peak in tropics/subtropics. Recent studies have suggested that absolute humidity (AH) had a U-shape relationship with influenza survival and transmission across climate zones, indicating that a unified influenza forecasting system could be established for China with various climate conditions.

Methods: Our study has generated weekly influenza forecasts by season and type/subtype in northern and southern China from 2011 to 2021, using a forecasting system combining an AH-driven susceptible-infected-recovered-susceptible (SIRS) model and the ensemble adjustment Kalman filter (EAKF). Model performance was assessed by sensitivity and specificity in predicting epidemics, and by accuracies in predicting peak timing and magnitude.

Results: Our forecast system can generally well predict seasonal influenza epidemics (mean sensitivity>87.5%; mean specificity >80%). The average forecast accuracies were 82% and 60% for peak timing and magnitude at 3–6 weeks ahead for northern China, higher than those of 42% and 20% for southern China. The accuracy was generally better when the forecast was made closer to the actual peak time.

Discussion: The established AH-driven forecasting system can generally well predict the occurrence of seasonal influenza epidemics in China.

* Corresponding author. School of Public Health, Fudan University, Key Laboratory of Public Health Safety, Ministry of Education, Xuhui District, Shanghai, 200231, China.
E-mail address: erinwang@fudan.edu.cn (X. Wang).
Peer review under responsibility of KeAi Communications Co., Ltd.

https://doi.org/10.1016/j.idm.2024.08.003

1. Introduction

Seasonal influenza is an acute respiratory infection resulting in 3–5 million severe cases and 290,000–650,000 deaths globally each year (Iuliano et al., 2018). Influenza usually exhibits a winter peak each year in temperate regions, but in tropical and subtropical regions it can have multiple peaks each year or circulate year-round (Tamerius et al., 2013). Accurate influenza forecasts have significant public health implications, which can provide valuable information in planning and deploying interventions such as the distribution of vaccines and antivirals.

Previous studies have suggested that meteorological factors were important to the seasonal circulation of influenza, especially temperature and relative humidity. Lowen et al. found that cold temperature and low relative humidity were favorable to the spread of influenza virus by a guinea pig model (Lowen et al., 2007). However, relative humidity is highly correlated with temperature. Shaman and Kohn reinterpreted Lowen's study in terms of absolute humidity (AH), which was the actual water vapor content of air irrespective of temperature (Shaman & Kohn, 2009). They found that the survival and transmission ability of influenza virus decreased with AH in a simple linear relationship, which was much stronger than the relationships with temperature or relative humidity. Therefore, Shaman et al. have developed an AH-driven forecast model which can generate accurate forecasts for temperate countries with peak timing and intensity accuracy exceeding 50% at 2–4 weeks prior to the actual peak time (Kramer & Shaman, 2019; Shaman & Karspeck, 2012).

However, as influenza activity is more irregular in tropical and subtropical regions, the model used in temperate regions is insufficient to explain the transmission patterns in tropics/subtropics. A few studies suggested that the effect of humidity on influenza transmission may follow a U-shape relationship rather than monotonically reduced, which implies that both low and high humidity conditions favor influenza transmission (Yang et al., 2012). Yuan et al. developed an AH-driven model with a U-shape relationship and reconstructed the long-term influenza epidemic dynamics in Hong Kong, which provided valuable evidence for influenza modeling in tropical and subtropical regions (Yuan et al., 2021).

China is a geographically, climatologically diverse country, and influenza seasonality varies significantly between northern and southern China (Bloom-Feshbach et al., 2013). It is challenging to forecast influenza activity in northern and southern China based on a unified forecasting system. Recently, an effort has been made by Zhanwei Du et al. (Du et al., 2023) to predict influenza incidence in China, but their model did not incorporate the meteorological driver. Our study aims to develop a unified AH-driven forecasting system to generate weekly forecasts of influenza for northern and southern China during the 2011–2021 seasons.

2. Materials and methods

2.1. Data

Weekly influenza surveillance data in northern and southern China from 2011 week 40 to 2021 week 40 were extracted from the Influenza Weekly Reports published by the Chinese National Influenza Center (CNIC, 2024). Northern and southern China were divided by the Qinling Mountains-Huaihe River Line (Shi et al., 2018). We used the product of weekly influenza-like illness (ILI) consultation rate and proportion of specimens tested positive for influenza as the influenza proxy (ILI+) (Yang et al., 2015). Daily mean temperature and relative humidity were collected from the China Meteorological Data Sharing Service System (http://data.cma.cn) and converted to weekly absolute humidity. Demographic data, including natural birth and death rates for 2011–2021 were obtained from the China Statistical Yearbook (http://www.stats.gov.cn/).

2.2. Definitions of seasonal epidemic

The baseline of seasonal influenza was defined as the 40% quantile of the non-zero ILI + records for each influenza type/subtype, or the first quartile of the non-zero ILI + records for all influenza types combined. The epidemic onset was defined as the first of three consecutive weeks with ILI + records exceeding a baseline, and the ending of an epidemic was defined as the first of two consecutive weeks with ILI + below the baseline following an onset. The period between an onset and its respective ending was defined as an epidemic duration (Yang et al., 2015). The peak timing was defined as the week with the maximum ILI+, and peak magnitude was defined as the maximum ILI+.

2.3. AH-driven forecasting system

We modeled influenza transmission using a susceptible-infected-recovered-susceptible (SIRS) model with demography. Absolute humidity modulates influenza transmission rates by altering basic reproductive number $R_0(t)$ through a U-shape relationship with both low and high AH conditions favoring influenza transmission (Yuan et al., 2021).

To forecast influenza activity, we combined the SIRS model with the ensemble adjustment Kalman filter (EAKF) to develop a SIRS-EAKF forecasting system. We first initialized the SIRS-EAKF system from a broad initial distribution for each parameter and performed two rounds of parameter optimization (Yuan et al., 2021) to generate parameter distributions that best fit the Chinese influenza activity (Supplementary Fig. S1).

Retrospective forecasting was then performed for northern and southern China, respectively. In northern China, the system was run by season and influenza type/subtype, generated forecasts at 6 weeks, 3 weeks, and 0 week before the actual

peak time. While in southern China, the system was run continuously from the first record to the last record and generated weekly 40-week forecasts. The SIRS-EAKF system was run with 300 ensemble members in both regions, and the system was reinitialized once filter divergence was detected (Yang et al., 2015). Details of the SIRS-EAKF system and the calculation of absolute humidity are presented in the Supplementary Material.

2.4. Model assessment

We first evaluated whether the forecast system can accurately predict upcoming epidemic events. A phase prediction was deemed accurate if the predicted epidemic trajectory included an epidemic during the predicted period. Similarly, it was deemed accurate if there was no predicted epidemic during a dormant period. Secondly, we assessed whether the forecast system can accurately predict the peak timing, peak magnitude, epidemic onset and duration. Predictions of epidemic onset or peak timing within ±1 week of observation, duration within ±2 weeks of observation, and peak magnitude within ±20% of the observation were deemed accurate. Thirdly, to further test whether our system outperformed a naive method, we conducted a simple analog forecast to predict the peak timing and magnitude (Yang et al., 2015). For each week, 100 forecasts were generated by randomly drawing peak timing and magnitude records from historical records. Forecast accuracy was tallied over all samples and compared to the AH-driven SIRS-EAKF method (Yang et al., 2015). The structure of SIRS-EAKF forecasting system was illustrated in Fig. 1.

3. Results

3.1. Influenza epidemics and impact of humidity on influenza transmission

We identified 11 influenza epidemics in northern China and 14 influenza epidemics in southern China during 2011–2021 seasons (Fig. 2). There were 7 A(H1N1),10 A(H3N2), and 8 influenza B epidemics in northern China, while the corresponding epidemics were 7, 10, and 8 in southern China. We found that R_0 was minimized when AH was in the range of 12.0–16.7 g/ m^3 (Table 1). R_0 increased quadratically with a decreasing AH up to a minimum of 2–8 g/m^3 and an increasing AH up to a maximum of 24–25 g/m^3 (Supplementary Fig. S2), confirming our assumptions of the U-shape relationship between AH and influenza transmission.

3.2. Reconstruction and forecasting ILI + time series

The AH-driven SIRS-EAKF system could well reconstruct the historical ILI + time series in northern and southern China with the mean correlation coefficients of 0.974 (95% CI: 0.970–0.978) and 0.983 (95% CI: 0.979–0.987), respectively. We found that the system could in general well predict the peak timing and magnitude over 3 weeks before the actual event in both northern and southern China. Forecast accuracy became higher when the prediction was made closer to the actual peak time. (Figs. 3 and 4).

3.3. Forecasting accuracy

In northern China, the forecast system could accurately detect an epidemic (mean sensitivity>95%) and did not falsely predict epidemics during dormant periods (mean specificity >85%) (Fig. 5A). Accuracies in southern China were slightly lower than those in northern China (mean sensitivity>80% and mean specificity >75%) but remained at a relatively high level. Forecasts for A(H3N2) and A(H1N1) had the highest sensitivity (100%), and forecasts for influenza B had the highest specificity (85%) in northern China. While in southern China, A(H1N1) had the highest sensitivity (90%) and specificity (87%).

The mean forecasting accuracy for peak timing in northern and southern China was 82% and 42% for 3–6 weeks before the actual peak time and increased to 99% and 97% for 3–6 weeks after the actual peak time (Fig. 5B & C). The mean forecasting accuracy for peak magnitude in northern and southern China was 60% and 20% for 3–6 weeks before the actual peak time and increased to 94% and 95% for 3–6 weeks after the actual peak time. However, the SIRS-EAKF system was unable to predict epidemic onset and duration prior to the actual peak time. In northern and southern China, the maximum accuracy for duration was 98% and 78% at 6 weeks after the actual peak time, while the accuracy of epidemic onset fluctuated around 20%.

Our forecasting system outperformed the simple analog forecast method (Supplementary Fig. S3). The accuracy of the SIRS-EAKF increased consistently as the forecast initiation time progressed (up to nearly 100%), while the accuracy of the naive method remained 20%–30% throughout the entire prediction period.

4. Discussion

Previous studies have found that real-time influenza forecasts could be generated using AH-driven predictive models in temperate countries (Shaman et al., 2013; Yang et al., 2014). However, due to the irregular influenza pattern in subtropical and tropical regions, few studies have been conducted to predict influenza activity accurately in these regions (Yuan et al., 2021; Du et al., 2023). For countries with complex climates such as China, it is difficult to build a unified national forecasting system. In this study, we constructed and tested an AH-driven forecasting system to handle the complex influenza dynamics in China.

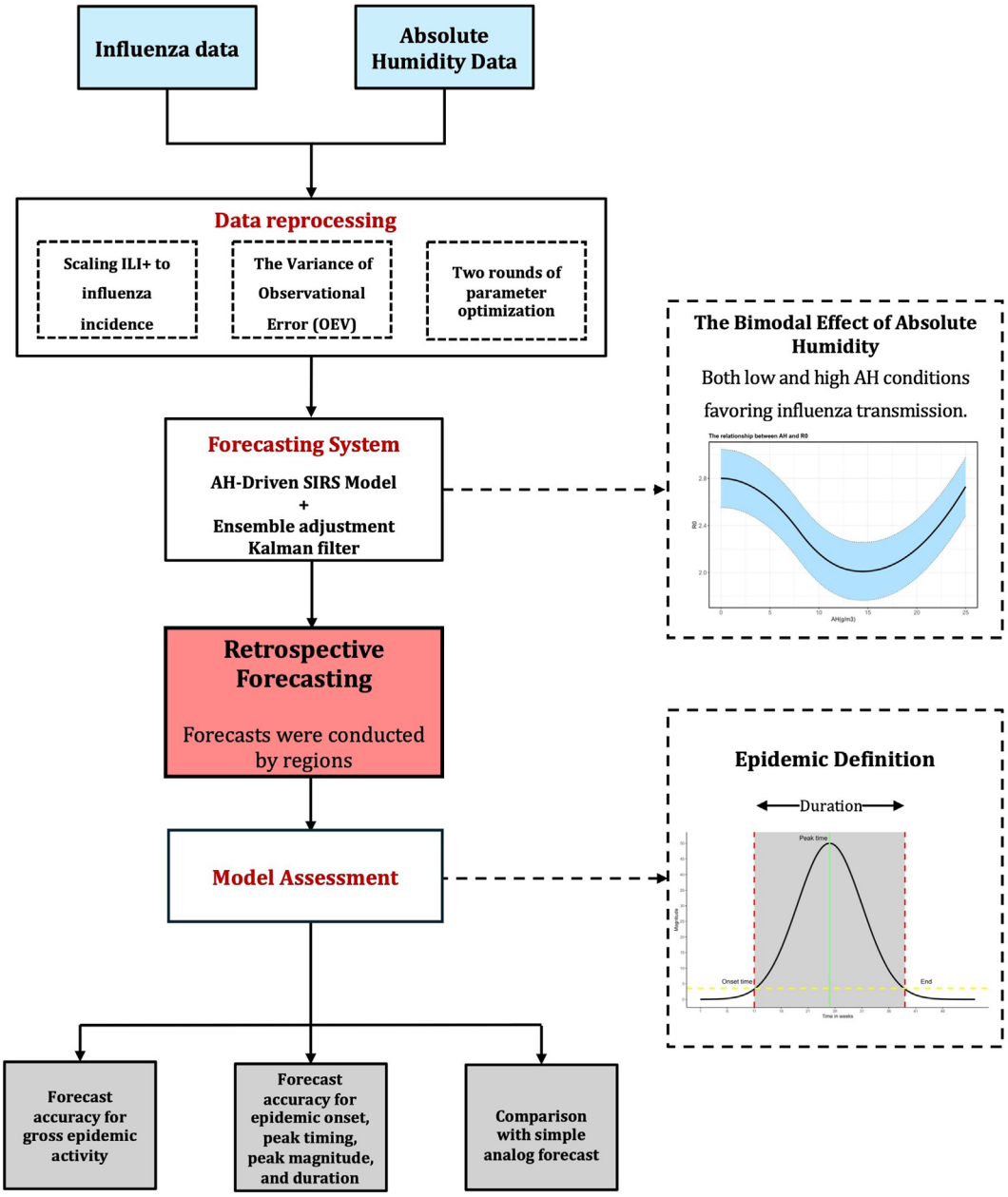

Fig. 1. The structure of SIRS-EAKF forecasting system.
Note: This figure illustrates the overall structure of the SIRS-EAKF forecasting system, including the processing of data, retrospective forecasting, and evaluation of the model.

Although many studies have suggested that the effect of humidity on influenza transmission may follow a U-shape relationship rather than monotonically reduced (Yang et al., 2012; Yuan et al., 2021), this effect has rarely been quantified or incorporated into influenza transmission models. In this study, we found the threshold of AH is approximately 12.0–16.7 g/m^3. Compared with the studies in Hong Kong (Yang et al., 2015) and Singapore (Tamerius et al., 2013), our AH threshold is slightly higher. This is mainly because these two studies were located in areas with lower latitudes, which had higher absolute humidity and more irregular influenza patterns. Moreover, recent studies have suggested that influenza transmission is driven by AH, moderated by temperature (Deyle et al., 2016). However, since the effect of temperature is currently unclear, we did not incorporate temperature into the model.

In the past decades, there has been a growing effort to develop systems and methods for forecasting different characteristics of influenza epidemics (Ali & Cowling, 2021). Qian et al. (*19*) used a seasonal autoregressive integrated moving

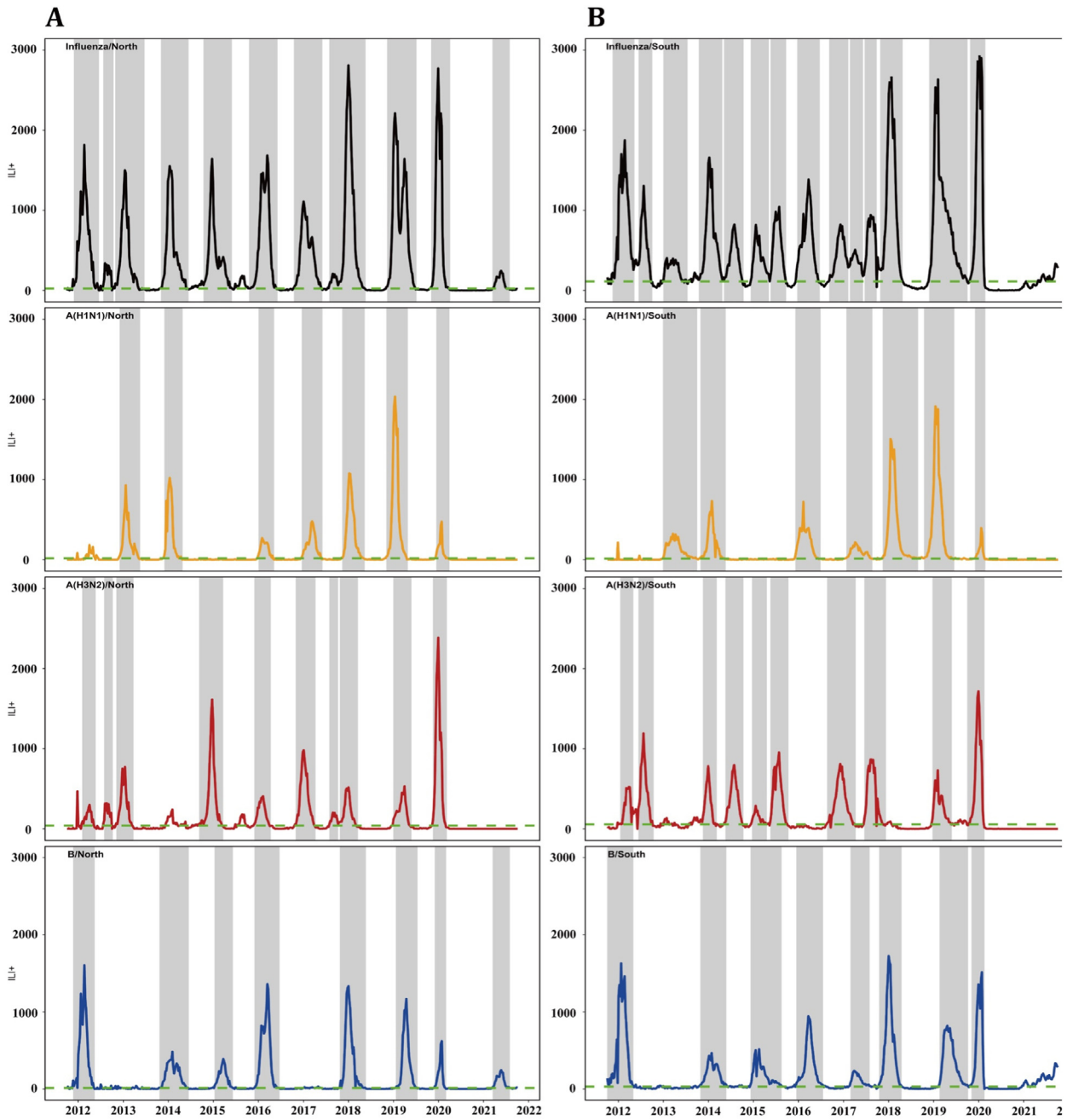

Fig. 2. Time series of ILI+ in northern (A) and southern (B) China, by type/subtype.
Note: The green horizontal line is the baseline; the grey shaded bars are epidemic periods. The baseline was defined as the 40% quantile of the non-zero ILI + records for each influenza strain, or the first quartile of the non-zero ILI + records for all influenza strains combined. The epidemic onset was defined as the first of three consecutive weeks with ILI + records exceeding a baseline, and the ending of an epidemic was defined as the first of two consecutive weeks with ILI + below the baseline following an onset.

average model (SARIMA) to predict the incidence trend of influenza-like illness proportion (ILI%) in Shanghai. Yang L et al. (Yang et al., 2024) recently built a deep-learning model upon Chinese influenza surveillance data to predict and provide early warnings for epidemic trends in China. Compared with these methods, the humidity-driven SIRS model used in this study is able to reflect the transmission dynamics of influenza viruses in populations in terms of the transmission mechanism, which can better predict the trend of influenza. In northern China, the system was run by seasons. While in southern China, the system was run continuously from the first record to the last record. The difference in forecast measurements is mainly due to

Table 1
Descriptions of the parameter ranges. The table lists all the variables and parameters used by the SIRS-EAKF system and their corresponding descriptions. The initial ranges and model estimation ranges for each variable and parameter are listed after them.

Parameter	Parameter Description	Initial ranges	Estimated ranges
N	The size of the model population.	100000	
$R_{0_{max}}$	The theoretical value of R_0 at $q = q_{min}$ and $q = q_{max}$.	1.5–3.5	2.4–3.0
$R_{0_{diff}}$	The difference between $R_{0_{max}}$, and R_0 at $q = q_{mid}$.	0.6–1.2	0.6–1.0
q_{min} (g/ m^3)	The absolute humidity value at which $R_0 = R_{0_{max}}$; the minimum value of absolute humidity permitted.	0–10	2.0–8.0
q_{max} (g/ m^3)	The absolute humidity value at which $R_0 = R_{0_{max}}$; the maximum value of absolute humidity permitted.	18–25	24.0–25.0
q_{mid} (g/ m^3)	The absolute humidity value at which $R_0 = R_{0_{max}} - R_{0_{diff}}$.	11.0–17.0	12.0–16.7
D (days)	The duration of influenza infection.	2–8	4–5
L (days)	The duration of influenza immunity.	150–3650	1275–1982
S_0	The number of people susceptible to influenza at the beginning of the model run.	40%N – 80%N	40305–48586
I_0	The number of people infected at the beginning of the model run.	10–500	28–425
p	An exponent to allow for imperfect mixing.	0.97	0.97

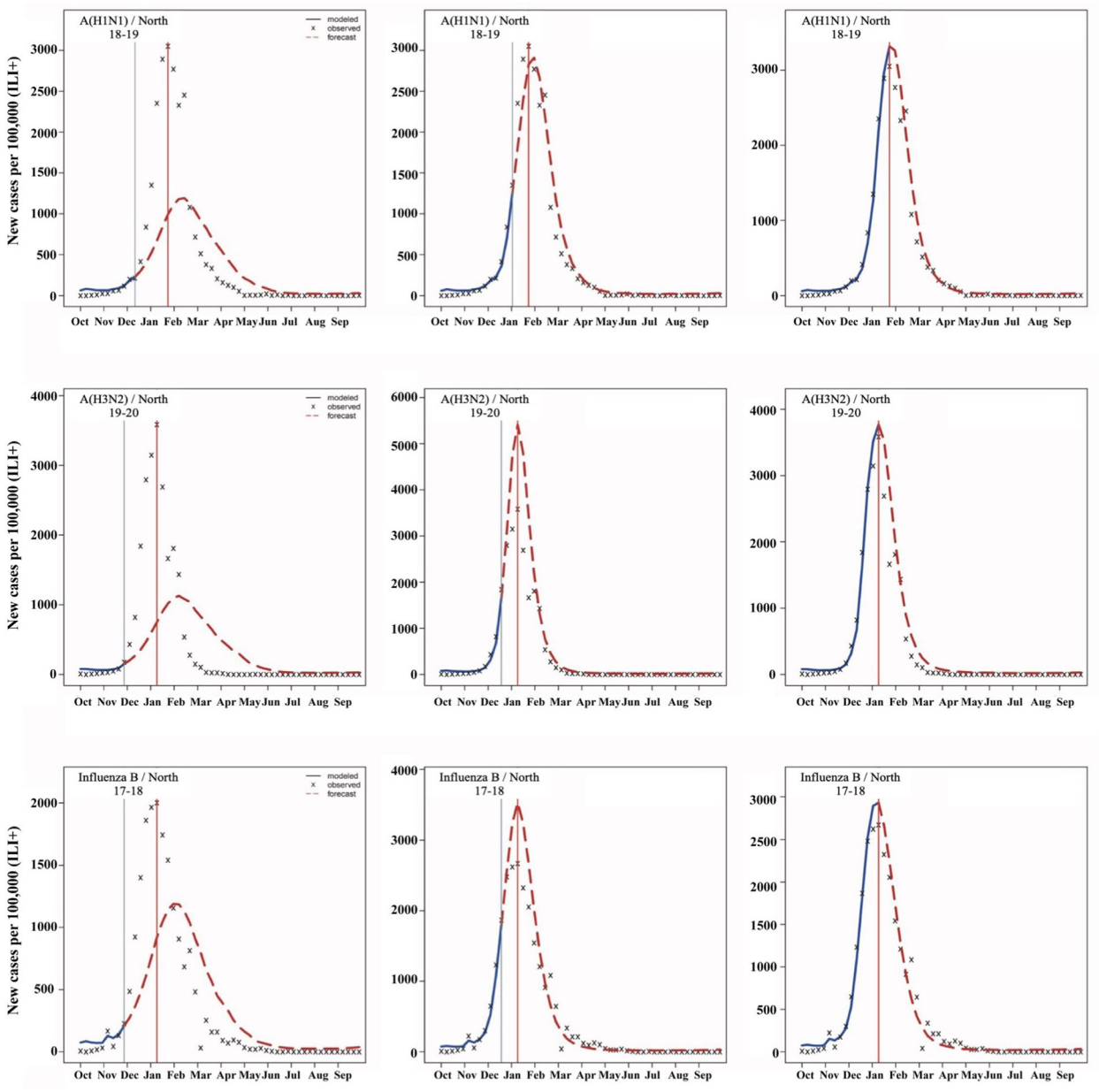

Fig. 3. Forecasted ILI + time series for A (H1N1), A(H3N2) and influenza B in northern China.
Note: The blue lines are modeled based on observations during the training period, and the red dashed lines are the forecasts generated by the system; red vertical lines indicate the actual peak time, and grey vertical lines mark the week the forecasts are made.

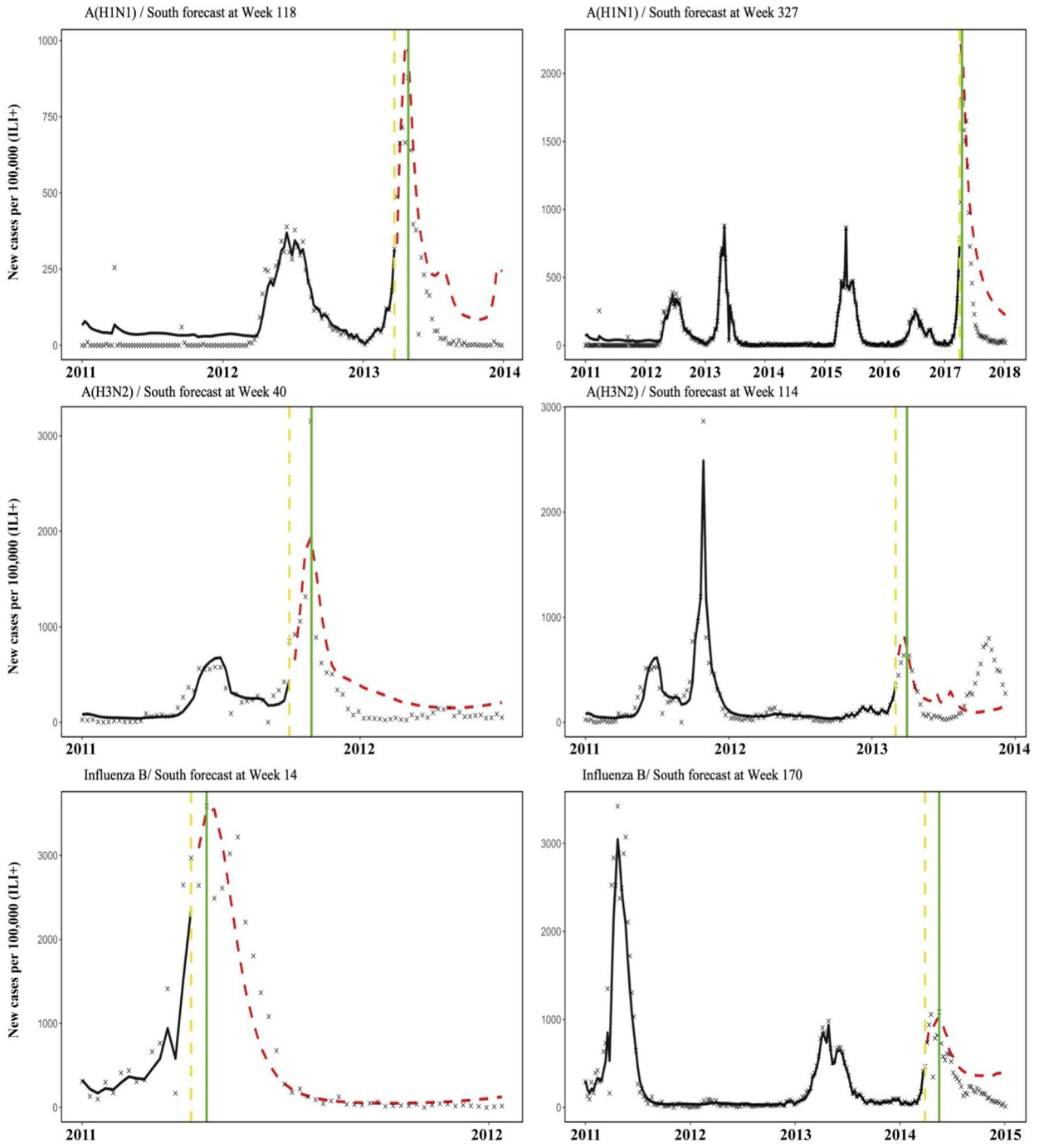

Fig. 4. Continuously forecasted ILI + time series in southern China.
Note: The 'x' points are the actual weekly ILI + data, the yellow vertical line is the start week of the forecast. The forecasting system was run continuously, the green vertical lines indicate the actual peak time, and the red dashed lines are forecasts for the next 40 weeks.

the irregularity of influenza activity in southern China, as dividing by seasons may cause some peaks in the southern China being separated into different seasons, thereby affecting the prediction accuracy. In addition to this, more detailed mechanistic models could be used in conjunction with the system as our understanding of influenza transmission dynamics improves in the future.

Notably, due to the strict non-pharmaceutical interventions (NPIs) implemented during the coronavirus disease 2019 (COVID-19) pandemic, influenza activity was significantly reduced in 2020 and 2021 seasons (Feng et al., 2021). Since the

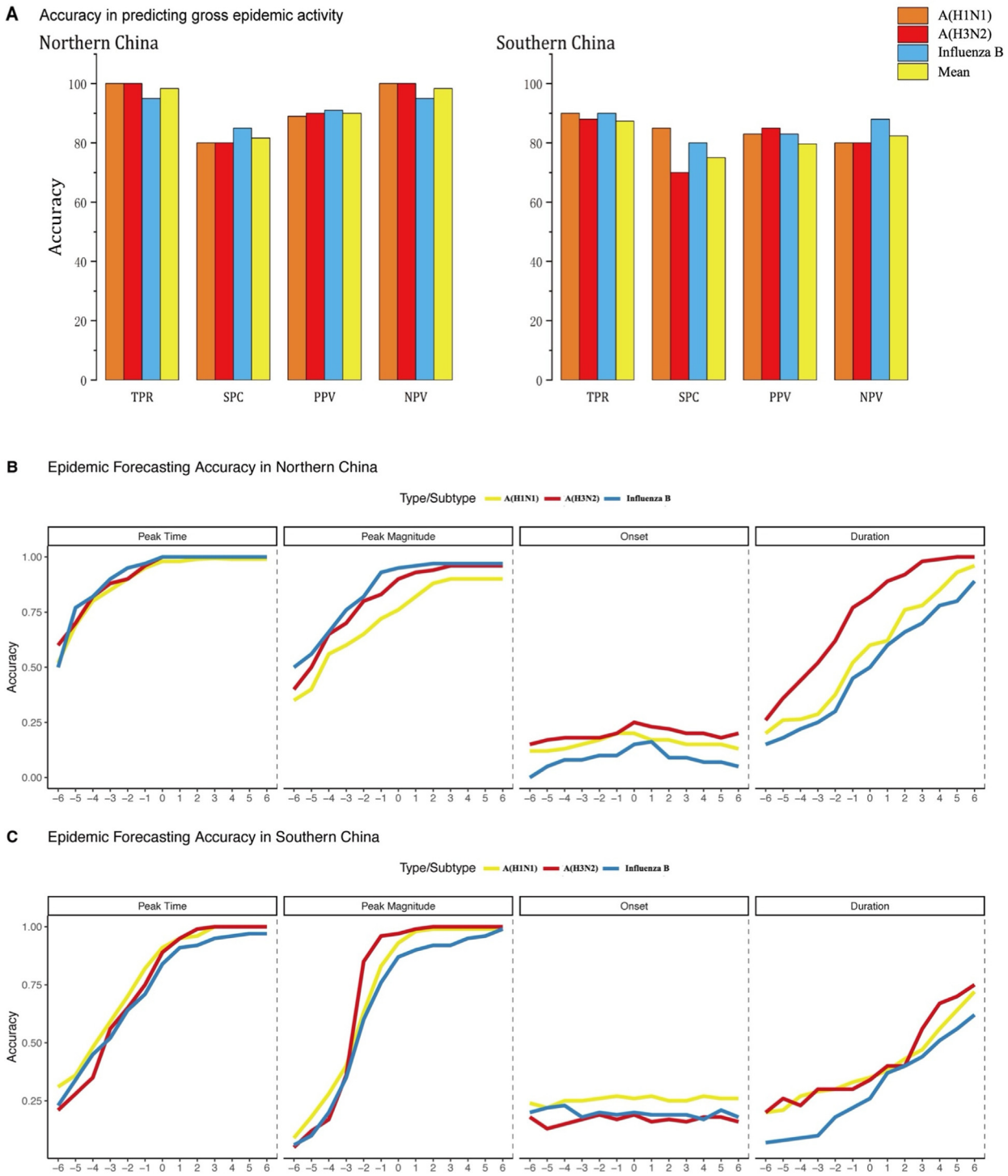

Fig. 5. Forecasting Accuracy of the system.
Note: (A) Four measures, sensitivity (TPR), specificity (SPC), positive predictive value (PPV), and negative predictive value (NPV) are shown for northern and southern China. Results are tallied over forecasts of each influenza type/subtype.
The accuracy in predicting peak timing, peak magnitude, epidemic onset and duration for each influenza type/subtype in northern (B) and southern (C) China. On the x-axis, positive leads indicate that the peak is in the past; negative leads indicate that the peak is in the future; a 0-week lead indicates that the peak is the same week as forecast. For example, "-6" means that the forecast starts at week 6 before the actual peak time, "6" means that the forecast starts at week 6 after the actual peak time, and "0" means that the forecast starts at the actual peak time.

interactive effect between influenza and SARS-CoV-2 is not well understood so far, we did not predict the influenza activity after the COVID-19 outbreak in this study. In the future, influenza and COVID-19 will co-exist in the population for a long time, further influenza prediction studies may need to consider the interaction between influenza and SARS-CoV-2 viruses.

The limitations of our study should be noted. Our model did not explicitly include the effects of contact patterns, vaccination, or NPIs. A more comprehensive model is needed in the future to optimize the forecasting ability of the system, especially in forecasting epidemic onset and duration (Yang et al., 2015).

In conclusion, our AH-driven forecasting system could generally well predict the occurrence of seasonal epidemics and generate reliable forecasts of peak timing and peak magnitude up to 3–6 weeks before the actual peak time. Our results suggested that a unified forecasting system of seasonal influenza for a large country with complex climate is possible. This system could provide reliable warnings of incoming influenza peaks and help public health workers in better anticipating influenza epidemics in forthcoming weeks.

Ethics approval

The research design and methodology used only publicly available data sets. This means that no ethical approval is required.

Funding

This work was supported by the Three-year Public Health System Construction Program of Shanghai, from Shanghai Municipal Health Commission of China [grant number GWV-10.2-YQ36].

Declaration of competing interest

The authors declare that they have no known competing financial interests or personal relationships that could have appeared to influence the work reported in this paper.

CRediT authorship contribution statement

Xiaowei Chen: Writing – original draft, Software, Formal analysis, Conceptualization. **Fangfang Tao:** Writing – review & editing. **Yinzi Chen:** Writing – review & editing. **Jian Cheng:** Writing – review & editing. **Ying Zhou:** Writing – review & editing. **Xiling Wang:** Writing – review & editing, Supervision, Project administration, Funding acquisition, Conceptualization.

Acknowledgments

This work was supported by the Medical Science Data Centre, Shanghai Medical College, Fudan University.

Appendix A. Supplementary data

Supplementary data to this article can be found online at https://doi.org/10.1016/j.idm.2024.08.003.

References

Ali, S. T., & Cowling, B. J. (2021). Influenza virus: Tracking, predicting, and forecasting. *Annual Review of Public Health, 42*, 43–57. https://doi.org/10.1146/annurev-publhealth-010720-021049

Bloom-Feshbach, K., Alonso, W. J., Charu, V., Tamerius, J., Simonsen, L., Miller, M. A., & Viboud, C. (2013). Latitudinal variations in seasonal activity of influenza and respiratory syncytial virus (RSV): A global comparative review. *PLoS One, 8*(2), Article e54445. https://doi.org/10.1371/journal.pone.0054445

CNIC. (2024). Weekly report. Retrieved Feb 14th from https://ivdc.chinacdc.cn/cnic/en/Surveillance/.

Deyle, E. R., Maher, M. C., Hernandez, R. D., Basu, S., & Sugihara, G. (2016). Global environmental drivers of influenza. *Proceedings of the National Academy of Sciences of the United States of America, 113*(46), 13081–13086. https://doi.org/10.1073/pnas.1607747113

Du, Z., Shao, Z., Zhang, X., Chen, R., Chen, T., Bai, Y., … Cowling, B. J. (2023). Nowcasting and forecasting seasonal influenza epidemics — China, 2022–2023. *China CDC Weekly, 5*(49), 1100–1106. https://doi.org/10.46234/ccdcw2023.206

Feng, L., Zhang, T., Wang, Q., Xie, Y., Peng, Z., Zheng, J., Qin, Y., Zhang, M., Lai, S., Wang, D., Feng, Z., Li, Z., & Gao, G. F. (2021). Impact of COVID-19 outbreaks and interventions on influenza in China and the United States. *Nature Communications, 12*(1), 3249. https://doi.org/10.1038/s41467-021-23440-1

Iuliano, A. D., Roguski, K. M., Chang, H. H., Muscatello, D. J., Palekar, R., Tempia, S., Cohen, C., Gran, J. M., Schanzer, D., Cowling, B. J., Wu, P., Kyncl, J., Ang, L. W., Park, M., Redlberger-Fritz, M., Yu, H., Espenhain, L., Krishnan, A., Emukule, G., … Mustaquim, D. (2018). Estimates of global seasonal influenza-associated respiratory mortality: A modelling study. *The Lancet, 391*(10127), 1285–1300. https://doi.org/10.1016/s0140-6736(17)33293-2

Kramer, S. C., & Shaman, J. (2019). Development and validation of influenza forecasting for 64 temperate and tropical countries. *PLoS Computational Biology, 15*(2), Article e1006742.

Lowen, A. C., Mubareka, S., Steel, J., & Palese, P. (2007). Influenza virus transmission is dependent on relative humidity and temperature. *PLoS Pathogens, 3*(10), 1470–1476. https://doi.org/10.1371/journal.ppat.0030151

Shaman, J., & Karspeck, A. (2012). Forecasting seasonal outbreaks of influenza. *Proceedings of the National Academy of Sciences of the United States of America, 109*(50), 20425–20430. https://doi.org/10.1073/pnas.1208772109

Shaman, J., Karspeck, A., Yang, W., Tamerius, J., & Lipsitch, M. (2013). Real-time influenza forecasts during the 2012–2013 season. *Nature Communications, 4*(1), 2837. https://doi.org/10.1038/ncomms3837

Shaman, J., & Kohn, M. (2009). Absolute humidity modulates influenza survival, transmission, and seasonality. *Proceedings of the National Academy of Sciences of the United States of America, 106*(9), 3243–3248. https://doi.org/10.1073/pnas.0806852106

Shi, Y., Wang, G., Gao, X., & Xu, Y. (2018). Effects of climate and potential policy changes on heating degree days in current heating areas of China. *Scientific Reports, 8*(1), Article 10211. https://doi.org/10.1038/s41598-018-28411-z

Tamerius, J. D., Shaman, J., Alonso, W. J., Bloom-Feshbach, K., Uejio, C. K., Comrie, A., & Viboud, C. (2013). Environmental predictors of seasonal influenza epidemics across temperate and tropical climates. *PLoS Pathogens, 9*(3), Article e1003194. https://doi.org/10.1371/journal.ppat.1003194

Yang, W., Cowling, B. J., Lau, E. H., & Shaman, J. (2015). Forecasting influenza epidemics in Hong Kong. *PLoS Computational Biology, 11*(7), Article e1004383. https://doi.org/10.1371/journal.pcbi.1004383

Yang, W., Elankumaran, S., & Marr, L. C. (2012). Relationship between humidity and influenza A viability in droplets and implications for influenza's seasonality. *PLoS One, 7*(10), Article e46789. https://doi.org/10.1371/journal.pone.0046789

Yang, W., Karspeck, A., & Shaman, J. (2014). Comparison of filtering methods for the modeling and retrospective forecasting of influenza epidemics. *PLoS Computational Biology, 10*(4), Article e1003583. https://doi.org/10.1371/journal.pcbi.1003583

Yang, L., Yang, J., He, Y., Zhang, M., Han, X., Hu, X., Li, W., Zhang, T., & Yang, W. (2024). Enhancing infectious diseases early warning: A deep learning approach for influenza surveillance in China. *Preventive Medicine Reports, 43*, Article 102761. https://doi.org/10.1016/j.pmedr.2024.102761

Yuan, H., Kramer, S. C., Lau, E. H. Y., Cowling, B. J., & Yang, W. (2021). Modeling influenza seasonality in the tropics and subtropics. *PLoS Computational Biology, 17*(6), Article e1009050. https://doi.org/10.1371/journal.pcbi.1009050